CHALMERS

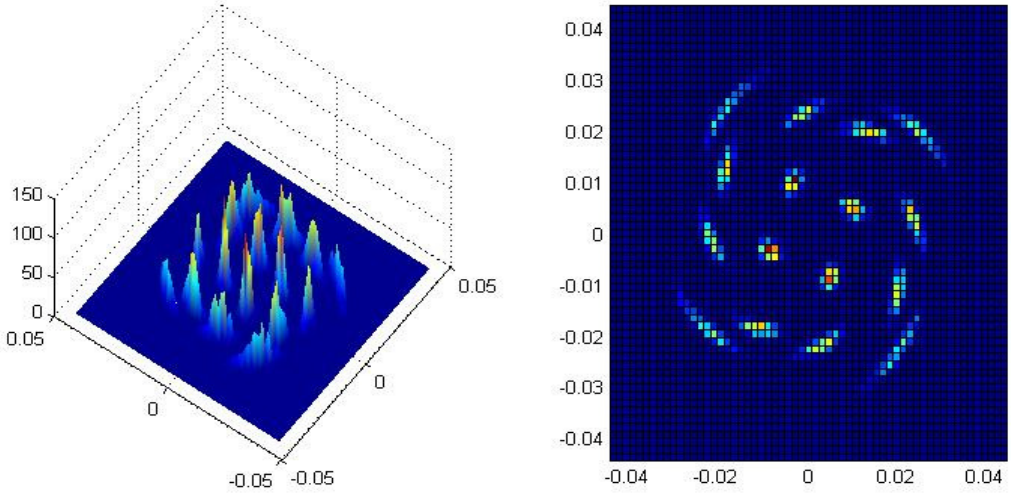

Nonlinear Phase Noise in Fiber Optical Communication

MOHSAN NIAZ CHUGHTAI

Communication Systems Group
Department of Signals and Systems
Chalmers University of Technology

Göteborg, Sweden, 2009 EX031/2009

ABSTRACT

Electronic compensation of nonlinear phase noise (NLPN) has been analyzed in the thesis work. Performance comparison of two methods to mitigate nonlinear phase noise has been carried out with Quadrature Amplitude Modulation (16 QAM) for data transmission in fiber optical communication. These methods focus on linear minimum mean square error (MMSE) minimization and optimal nonlinear post compensation.

In the previous results, the best system performance is achieved by nonlinear post compensation with uniformly distributed phase 16 QAM constellation. The performance of nonlinear post compensation is further improved by optimization of 16-QAM constellation which has four shells with uniform distribution of radii. Each shell has four points with uniformly distributed phases.

With the proposed constellation the complexity of the receiver remains unchanged and it becomes more immune to nonlinear phase noise at higher transmission powers. The optimum launch power is increased by 2 dB with reduction of SER to about 10^{-8}. With this improvement the transmission distance of the system is also increased from 3000 km to 3540 km at the previous minimum SER of 10-6. So in terms of transmission distance the system has an improvement of 540 km.

ACKNOWLEDGEMENTS

The thesis work was carried out in the Signals and Systems Department, Chalmers University of Technology, under the supervision of Lotfollah Beygi and examination of Associate Professor Dr. Erik Agrell.

I would like to thank PhD Student Lotfollah Beygi for his encouragement during the entire period of the thesis work to push the work further and achieve new results. Then I would also like to thank Associate Professor Dr. Erik Agrell whom has guided me with very important advices not only during the thesis work but also during my entire Masters programme's period.

Another important contribution was the guidance from Dr. Mats Sköld from the Photonics laboratory of the Micro Technology and Nano Science Department of Chalmers University of Technology. His help has been very important in understanding the practical aspects of the fiber optical communication systems.

Then at last I would like to thank Dr Pontus Johannisson from the Photonics laboratory of the Micro Technology and Nano Science Department of Chalmers University of Technology for his special interest and guidance in the thesis work.

TABLE OF CONTENTS

CHAPTER 1

INTRODUCTION

The evolution of advanced digital modulation schemes such as Quadrature Phase Shift Keying (QPSK) and Quadrature Amplitude Modulation (QAM) in wireless and land line communications have attracted significant importance as new alternatives to boost the capacity of fiber optical communication systems.

But with every new alternative come new limitations. Fiber optical communication channels are limited by linear and nonlinear impairments. Linear impairments include chromatic dispersion (CD) and polarization mode dispersion (PMD).

Nonlinear impairments originate from the variation of the refractive index of the optical fiber dependent on the launched power. This phenomenon is called Kerr effect named after the Scottish Physicist John Kerr. Nonlinear impairments include self phase modulation (SPM), cross phase modulation (XPM) and four wave mixing (FWM).

Specifically SPM causes the signal travelling through the fiber to change its own phase. In the case of optically amplified fiber optical communication links, noise introduced by erbium doped fiber amplifiers (EDFA) causes the self phase modulation to change in a random fashion and is referred to as nonlinear phase noise (NLPN) which has been mathematically analyzed in the initial chapters 2 and 3.

Since information in advanced digital modulation formats is encoded in both phase and amplitude, NLPN becomes a dominant source of symbol errors during demodulation at the receiver. Therefore the integration of digital modulation formats in fiber optical communication requires modifications in digital modulation schemes and the compensation of NLPN and other optical impairments at both transmitter and receiver.

In recent years the increasing speed of digital signal processors has made possible the compensation of optical impairments in the electronic domain, very cost effective. Thus various signal processing algorithms, both new and existing, are being proposed to compensate optical impairments in the electronic domain.

Techniques to mitigate NLPN in electronic domain have been proposed based on minimization of variance of NLPN. Earlier works have been focused entirely on the analysis of NLPN compensation for binary phase shift keying (BPSK) and Quadrature Phase Shift keying (QPSK) modulation studied in chapter 4. In this thesis work performance of a fiber optical communication system with 16 QAM modulation and NLPN compensation has been analyzed in last chapter 5 which also contains the discussion of the simulations and the contribution made to previously obtained results.

CHAPTER 2

LINEAR PHASE NOISE

In every communication system, the channel has impacts on the signal travelling through it. One of the most common impacts is the Additive White Gaussian Noise (AWGN) added to the signal. This noise impacts the signal equally in all degrees of freedom in which the signal is defined thus changing the phase and amplitude of the received signal in a random fashion and having a specific distribution.

2.1. AMPLIFIED SPONTANEOUS EMISSION NOISE

Amplified spontaneous emission (ASE) noise in the EDFAs is due to spontaneous emission of photons generated from inversion of electrons from the Meta stable state to the stable state. These spontaneously generated photons are also amplified within the amplifier and thus act as noise source in the system. The power spectral density of ASE noise is given by [1 p.188-189]

$$S_{ASE}(\nu_o) = (G-1)\,\eta_{sp}\,h\nu_o$$

where ν_o is the central frequency, G is the gain of the amplifier, h is the Planck's constant, η_{sp} is the spontaneous emission factor defined below

$$\eta_{sp} = \frac{N_2}{N_2 - N_1}\ ,$$

where N_2 and N_1 are the atomic populations for the excited and ground states.

When an optical band pass filter is used before the receiver the power of ASE noise is limited to the bandwidth of the filter. A signal travelling in fiber optical channels has two states of polarization. ASE noise acts in the two polarizations independently thus increasing the power spectral density of ASE noise by a factor of two. The power spectral density or the variance of ASE noise is given as follows:

$$P_{ASE} = 2\int_{-\infty}^{\infty} S_{ASE} H_f(\nu - \nu_o)\,d\nu \approx 2S_{ASE}\Delta\nu_o$$

where H_f is the transfer function of the optical band pass filter and $\Delta\nu_o$ is the effective bandwidth of the optical filter. The power spectral density is considered to be almost flat with in the bandwidth of the optical filter so ASE noise is AWGN with mean zero and variance P_{ASE} .

2.2. LINEAR PHASE NOISE IN FIBER OPTICAL COMMUNICATION LINK

The total received phase of PSK sytems is given by

$$\phi_r = \theta_o + \theta_n$$

where ϕ_r is the total is received phase, θ_o is the transmitted phase and θ_n is the linear phase noise due to ASE noise. The distribution of linear phase noise can be approximated by [2, p.139]

$$p_{\theta_n}(\theta_n) \approx \sqrt{\frac{\rho_s}{\pi}} \cos\theta_n e^{-\rho_s \sin^2 \theta_n}$$

where ρ_s is the optical signal to noise ratio (OSNR) defined below

$$\rho_s = \frac{A^2}{2N_A\sigma^2}$$

where A is the transmitted amplitude, N_A is the number of amplifiers in the system and σ^2 is the variance of ASE noise from EDFAs. The variance of linear phase noise is given as

$$\sigma^2_{\theta_n} \approx \frac{1}{2\rho_s}.$$

The distribution of phase noise can also be approximated by Gaussian distribution given below by [2, p.139]

$$p_{\theta_n}(\theta_n) \approx \sqrt{\frac{\rho_s}{\pi}} \exp\left[-\theta_n{}^2 \rho_s\right].$$

2.3. SYMBOL ERROR PROBABILITY OF PSK SYSTEM

The probability of symbol error for an *M-ary* PSK system is related to linear phase noise by the following expression [3, p.226]

$$P_e = 1 - \int_{-\pi/M}^{\pi/M} p_{\theta_n} d\theta_n$$

which gives the following expression

$$P_e \approx 2Q\left(\sqrt{2\rho_s}\sin\frac{\pi}{M}\right)$$

where M is the modulation level. It is plotted in figure 1 on the next page.

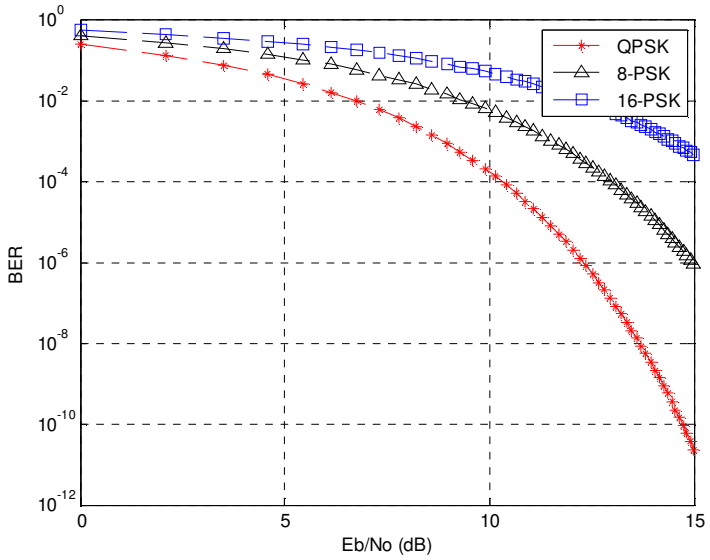

Figure 1: Probability of bit error for various modulation schemes.

CHAPTER 3

NONLINEAR PHASE NOISE

3.1. OPTICAL KERR EFFECT

Optical Kerr effect was discovered by a Scottish physicist in 1875 John Kerr. Optical Kerr effect or AC Kerr effect causes the refractive index of the material to change in proportion to the intensity or power of the electromagnetic field. The change in refractive index is as follows [4]:

$$\Delta n = n_2 \left(\frac{P}{A_{eff}} \right)$$

where n_2 is the nonlinear refractive index, P is the launched power and A_{eff} is the effective core area of the optical fiber. This change in refractive index is responsible for the signal to change its own phase i.e., self phase modulation.

3.2. SELF PHASE MODULATION

The mathematical equation governing the propagation of light in optical fibers is the nonlinear Schrödinger equation given as follows [1, p.108]:

$$\frac{\partial A}{\partial z} + \frac{i\beta_2}{2}\frac{\partial^2 A}{\partial t^2} = i\gamma |A|^2 - \alpha \frac{A}{2}$$

where A is launched amplitude, z is the distance, t is time, α is the attenuation coefficient, γ is the nonlinear parameter defined as

$$\gamma = \frac{2\pi n_2}{\lambda_o A_{eff}}$$

where λ_o is the central wavelength, n_2 is the nonlinear refractive index, and A_{eff} is the effective core area. The solution to the nonlinear Schrödinger equation when $\beta_2 = 0$, which governs dispersion, is given below

$$A(z,t) = A(0,t)\exp[i\phi_{NL}(z,t)]$$

where $A(z,t)$ is the amplitude of signal pulse as a function of distance and time

and ϕ_{NL} is given as

$$\phi_{NL} = \gamma \int_0^L |A(0,t)|^2 dz$$

$$\phi_{NL} = \gamma L_{eff} |A(0,t)|^2 \quad (1)$$

where $$L_{eff} = \int_0^L e^{-\alpha z} dz = N_A[1 - e^{-\alpha L_A}]/\alpha \approx N_A/\alpha$$

is the effective length of a link with N_A amplifiers spaced at distance of L_A .

The expression (1) indicates that the phase modulation is directly proportional to the instantaneous power of the signal being transmitted. Figure 2 illustrates self phase modulation. The first curve shows pulse amplitude and the second curve shows the deviation of frequency from the central frequency. The second curve is the derivate of the first curve since frequency is time derivate of phase change and phase change is directly proportional to the instantaneous amplitude. This discussion is mathematically summarized as follows [1, p.109]:

$$\delta\omega(t) = -\frac{\partial \phi_{NL}}{\partial t} = -\gamma L_{eff} \frac{\partial}{\partial t} |A(0,t)|^2 .$$

where $\delta\omega(t)$ is the deviation from the central frequency of the system.

3.3. SPM IN AMPLIFIED FIBER OPTICAL COMMUNICATION LINK

In the context of phase modulated and amplified optical communication links the interplay of amplified spontaneous emission noise and Kerr effect causes the received constellation to rotate in a random fashion and is referred as Gorden-Mollenauer effect. [5] For long haul fiber optical communication (FOC) links with cascaded EDFAs, the NLPN added into the system, is expressed mathematically as follows [6]:

$$\phi_{NL} = \gamma L_{eff} \{ |A + n_1|^2 + |A + n_1 + n_2|^2 + |A + n_1 + n_2 + n_3|^2 + ... + |A + n_1 + n_2 + n_3 + ... + n_{N_A}|^2 \} \qquad (2)$$

where A is the amplitude of the transmitted signals and $n_k, k = 1, ..., N_A$ are the noise terms that have chi squared distribution with two degrees of freedom since noise affects both the In-phase and Quadrature components of the signal. The variance of n_k is $\langle |n_k|^2 \rangle = 2\sigma^2$.

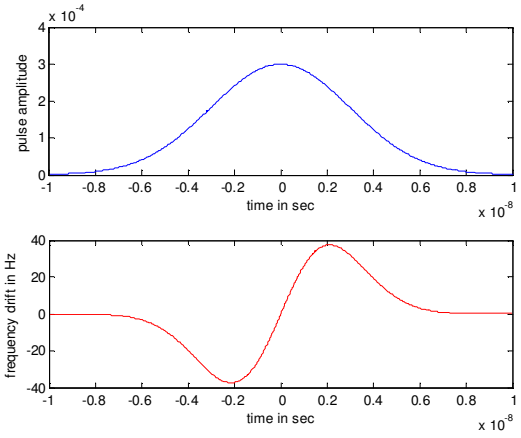

Figure 2: Frequency shift $\delta\omega(t)$ due to self phase modulation.

Analysis of the expression (2) shows that the process of addition of nonlinear phase noise is a nonlinear time dependent process opposite to that of a linear time independent process. This is because once NLPN is added in the system it remains in the system till it reaches the receiver for demodulation.

Figure 3 shows the process of evolution of NLPN as a BPSK signal is being propagated through the fiber. Figure 3(a) shows the probability density function (PDF) of scatter plot when the mean nonlinear phase shift is 0.7 radians and figure 3(b) shows the PDF of scatter plot when the mean nonlinear phase shift is 1.5 radians. This shows that as the signal propagates the mean nonlinear phase shift increases as well as the variance of the NLPN also increases.

3.4. STATISTICS OF NLPN

The term $|A+n_1|^2$ in expression (2) has a non central chi squared distribution with two degrees of freedom. So the mean and variance of $|A+n_1|^2$ is given as follows [6]:

$$\left\langle |A+n_1|^2 \right\rangle = A^2 + 2\sigma^2$$

$$\sigma^2_{\{|A+n_1|^2\}} = f(\sigma^2) = 4A^2\sigma^2 + 4\sigma^4 .$$

The covariance between the two terms in expression (2) is given by

$$Cov(|A+n_1|^2, |A+n_1+n_2|^2) = f(\sigma^2) = 4A^2\sigma^2 + 4\sigma^4 .$$

So the total variance of expression (2) can be expressed as follows:

$$\sigma^2_{NL} = (\gamma L_{eff})^2 \left[\sum_{K=1}^{N_A} f(K\sigma^2) + 2\sum_{K=1}^{N_A} (N_A - K) f(K\sigma^2) \right]$$

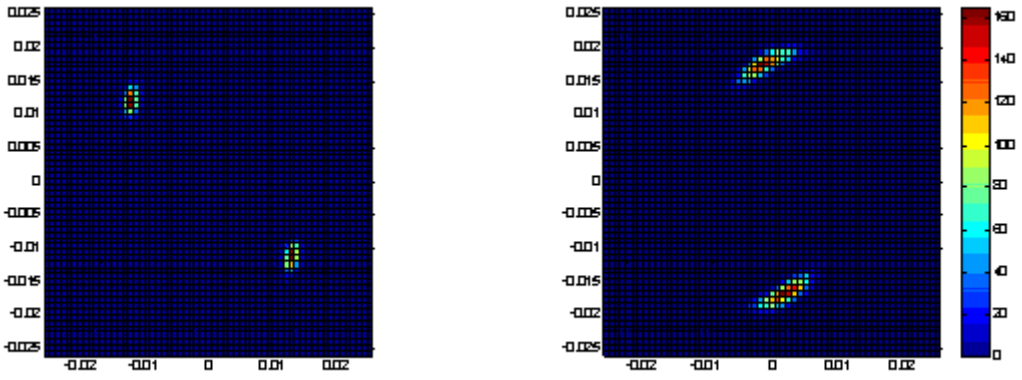

(a) (b)

Figure 3: PDF of received BPSK signal with NLPN for mean nonlinear phase shift of (a) 0.7 radians after 2000 km (b) 1.5 radians after 4000 km for a transmitted power of -5 dBm.

which by using mathematical induction gives the following expression

$$\sigma_{\phi_{NL}}^2 = \frac{2}{3}N(N+1)(\gamma L_{eff}\sigma)^2\left[(2N+1)A^2 + (N^2+N+1)\sigma^2\right].$$

The variance of nonlinear phase noise can be related to OSNR by the following relation

$$\sigma_{\phi_{NL}}^2 \approx \frac{2\langle\phi_{NL}\rangle^2}{3\rho_s}.$$

The mean of NLPN is expressed as follows:

$$\langle\phi_{NL}\rangle = N_A\gamma L_{eff}[|A|^2 + (N_A+1)\sigma^2] \approx N_A\gamma L_{eff}|A|^2.$$

At first glance, from central limit theorem, it seems that nonlinear phase noise should have a Gaussian distribution but this is not the case since the random NLPN at every amplifier stage is correlated to the NLPN in the previous amplifier stages. Expression (2) can be expressed in form of a matrix as follows [2, p. 148-150]:

$$\phi_{NL} = N_A A^2 + 2Aw^T x + x^T C x \tag{3}$$

where $w = [N_A, N_A - 1, ..., 2, 1]^T$ and $x = [n_1, n_2, ..., n_{N_A}]^T$

and C is the covariance matrix which is a product of the two matrices defined as $C = MM^T$,where M is as follows:

$$M = \begin{bmatrix} 1 & 0 & 0 & \cdots & 0 \\ 1 & 1 & 0 & \cdots & 0 \\ 1 & 1 & 1 & \cdots & 0 \\ \vdots & \vdots & \vdots & \ddots & \vdots \\ 1 & 1 & 1 & \cdots & 1 \end{bmatrix}.$$

The exact PDF of the NLPN is difficult to compute so it is computed by taking the inverse Fourier transform of the characteristic function of expression (3) which is given by [2, p.150]

$$\Psi_{\phi_{NL}}(jv) = \prod_{K=1}^{N_A}\frac{1}{1-2jv\sigma^2\lambda_k}\exp\left[\frac{jvA(\underline{v}_k^T w)^2/\lambda_k}{1-2jv\sigma^2\lambda_k}\right]$$

where $\underline{v}_k^T$ and λ_k are eigen vectors and eigen values of the covariance matrix C.

The characteristic function is further simplified by expressing NLPN as normalized NLPN given as follows [7]:

$$\Psi_{\phi}(jv) = \sec\sqrt{jv}\exp[\rho_s\sqrt{jv}\tan\sqrt{jv}]$$

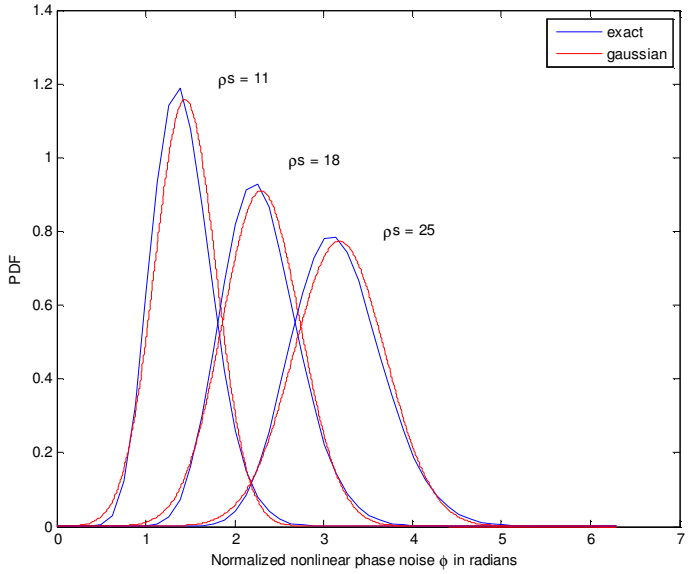

Figure 4: PDF of Normalized nonlinear phase noise ϕ for various OSNRs.

where scaling from normalized nonlinear phase noise to nonlinear phase noise is defined as

$$\phi_{NL} = \frac{\langle \phi_{NL} \rangle}{\rho_s + 0.5} \phi$$

where ϕ is the normalized nonlinear phase shift and ρ_S is the OSNR.

A comparison between actual and Gaussian approximation of the NLPN is shown in figure 4 which indicates that the exact distribution of NLPN is not Gaussian but very near to it.

3.5. SYMBOL ERROR PRORBABILTY OF PSK SYSTEM IN NLPN

The total received phase of PSK sytems is given by [8]

$$\phi_r = \theta_o + \theta_n + \phi_{NL}$$

where θ_o is the transmitted phase, θ_n is the linear phase noise and ϕ_{NL} is the nonlinear phase noise. The total received phase can also be expressed in terms of normalized NLPN.

$$\phi_r = \theta_o + \theta_n + \frac{\langle \phi_{NL} \rangle}{\rho_s + 0.5} \phi .$$

Now considering that the transmitted phase θ_o is zero then received phase can be expressed as follows:

$$\phi_r = \theta_n + \frac{\langle \phi_{NL} \rangle}{\rho_s + 0.5} \phi .$$

The characteristic function of linear phase noise can be calculated from

$$\Psi_{\theta_n}(jv) = \int_{-\pi}^{\pi} p_{\theta_n}(\theta_n) e^{-jv\theta_n} d\theta_n$$

where $p_{\theta_n}(\theta_n)$ is the PDF of linear phase noise defined earlier in section 2.2. The PDF of total received phase signal is the inverse Fourier transform of the product of characteristic functions of linear and nonlinear phase noise given by.

$$\Psi_{\phi_r}(jv) = \Psi_{\theta_n}(jv)\Psi_{\phi_{NL}}\left(-jv\frac{\langle\phi_{NL}\rangle}{\rho_s + 0.5}\right)$$

where $\Psi_{\phi_{NL}}$ is the characteristic function of nonlinear phase noise defined in section 3.4. The PDF of total received phase is the inverse Fourier transform of the above given by

$$p_{\phi_r}(\phi_r) = \frac{1}{2\pi}\int_{-\infty}^{\infty} \Psi_{\phi_r}(jv) e^{jv\phi_r} d\phi_r .$$

The probability of error for a binary phase shift keying (BPSK) system is calculated by following expression

$$Pe = 1 - \int_{-\pi/2-\langle\phi_{NL}\rangle}^{\pi/2-\langle\phi_{NL}\rangle} p_{\phi_r}(\phi_r) d\phi_r .$$

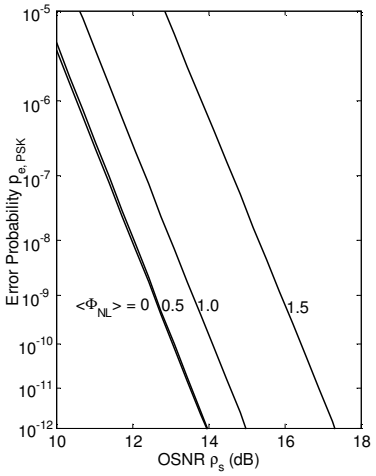

Figure 5: Symbol error rate for BPSK signal as a function of OSNR. ([8]; reprinted with permission)

Figure 5 shows the plot for probability of bit error as a function of optical signal to noise ratio (OSNR) for various mean nonlinear phase shifts. The plot depicts the increase in error probability as the mean nonlinear phase shift increases.

3.6. JOINT PDF OF NLPN AND RECEIVED AMPLITUDE

The joint PDF of received phase θ and amplitude *r*, for a transmitted power P and phase θ_o is given as follows [9]:

$$f_{P,\theta_o}(r,\theta) = \frac{f_R(r,P)}{2\pi} + \frac{1}{\pi}\sum_{m=1}^{\infty} \mathrm{Re}\left\{C_m(r)e^{jm(\theta-\theta_o)}\right\}. \quad (4)$$

The first expression is the PDF of received amplitude for transmitted amplitude R and power P which is given by Rice distribution as follows:

$$f_R(r,P) = 2re^{-(r^2+P/\sigma^2)} + I_o(2r\sqrt{P/\sigma^2})$$

where $C_m(r)$ is defined as

$$C_m(r) = \frac{r\sec\sqrt{jmx}}{s_m} e^{\rho_s\sqrt{jmx}\tan\sqrt{jmx}} e^{-\frac{r^2+\alpha_m^2}{2s_m}} I_m\left(\frac{\alpha_m r}{s_m}\right)$$

where I_m is the m^{th}-order modified Bessel function of the first kind and

$$x = \frac{\gamma PL}{\rho_s + 0.5}\ , \alpha_m = \sqrt{\rho_s}\sec\sqrt{jmx}\ ,\ s_m = \frac{\tan\sqrt{jmx}}{2\sqrt{jmx}}\ .$$

CHAPTER 4

COMPENSATION OF NLPN

4.1. DIGITAL BACK PROPAGATION

Digital back propagation has been proposed for joint mitigation of SPM and chromatic dispersion [10]. Digital back propagation is based on the nonlinear Schrödinger equation given as follows:

$$\frac{\partial A}{\partial z}+\frac{i\beta_2}{2}\frac{\partial^2 A}{\partial t^2}+\frac{\alpha}{2}A=i\gamma|A|^2 A.$$

Nonlinear Schrödinger equation is invertible and can be expressed as

$$\frac{\partial A}{\partial z}-\frac{i\beta_2}{2}\frac{\partial^2 A}{\partial t^2}-\frac{\alpha}{2}A=-i\gamma|A|^2 A$$

$$\frac{\partial A}{\partial z}=\left(N'+D'\right)A$$

where N' and D' are defined as $N'=i\gamma|A|^2$

$$D'=-\frac{i\beta_2}{2}\frac{\partial^2}{\partial t^2}-\frac{\alpha}{2}.$$

So the receiver can be designed based on reverse NLSE in which the received signal can be reverse propagated through a filter with opposite signs of α, β_2 and γ for the joint mitigation of NLPN and chromatic dispersion.

4.2. SPLIT STEP FOURIER METHOD

Split step Fourier method (SSFM) is used to simulate self phase modulation and chromatic dispersion in fiber optical communication simultaneously. In the split step Fourier method nonlinearity acts on the signal alone in time domain then Fourier transform is applied to the signal. In the second step, dispersion is applied in the frequency domain by replacing the $\partial/\partial t$ in nonlinear Schrödinger equation by $i\omega$. Finally the signal is retrieved by taking the inverse Fourier transform of the signal. The overall operation can be expressed as follows [11]:

$$A(z+h,t)=F^{-1}[e^{hD(i\omega)}F[e^{hN}A(z,t)]]$$

where F is the Fast Fourier transform (FFT) operation and h is the small incremental distance.

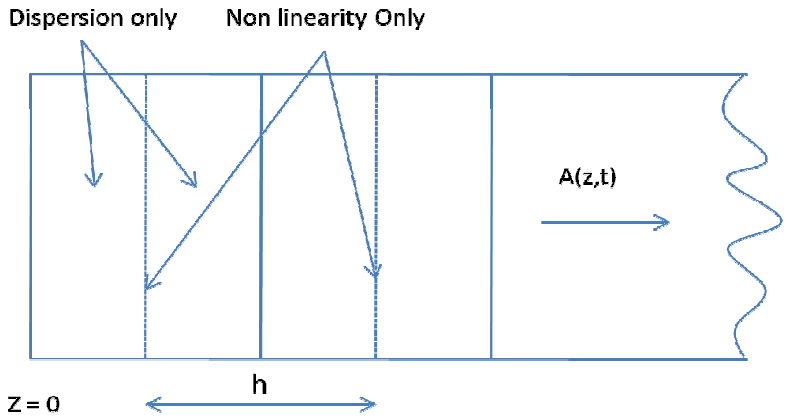

Figure 6: Illustration of symmetric split Fourier method.

4.3. ITERATIVE AND SYMMETRIC SPLIT STEP FOURIER METHOD

In this method the signal is propagated through half of the distance `h´ with dispersion acting on it and then at middle of the distance nonlinearity acts on it and then in the remaining half of the distance dispersion acts on it again depicted in the figure 6. The process is approximated by the following equation [12, p.42-44]:

$$A(z+h,t) = \exp\left(\frac{h}{2}D\right)\exp\left(\frac{N(z)+N(z+h)}{2}\right)\exp\left(\frac{h}{2}D\right)A(z,t)$$

In the case of an amplified optical communication link, for each span between amplifiers several iterations, according to the number of divisions `h´, have to be performed for the mitigation of nonlinearity and dispersion, leading to a very high complexity.

4.4. NONITERATIVE ASYMETRIC SPLIT STEP FOURIER METHOD

Simplification of the above mentioned method is done by assuming that nonlinearity is only concentrated at the beginning of each amplifier link hence only one iteration is performed for each span of fiber thus greatly reducing the complexity of the system for mitigation of nonlinear phase noise. [10]

The performance of noniterative asymmetric SSFM is 2 to 3 dB poor than iterative symmetric SSFM but the computations are fewer as only one iteration has to be performed for every span of the link. SSFM is indeed quite a powerful method to mitigate both nonlinearity and dispersion yet it still has a high computational cost of approximately 10^5 multiplications per symbol per channel. [13]

4.5. LINEAR MMSE BASED COMPENSATION

The received power in an amplified fiber optical communication link is $P_N = |A + n_1 + n_2 \ldots\ldots + n_{N_A}|^2$ which is also the last term in expression (2) of NLPN and the only quantitative information at receiver about the NLPN added to the signal. Nonlinear phase noise can then be compensated at the receiver by subtracting a phase proportional to P_N from the received signal phase.

The compensated phase is $\phi_r - \alpha P_N$, where ϕ_r is the received phase, α is the optimal compensating factor that minimizes the variance of residual nonlinear phase noise calculated by $d\sigma^2_{\phi_{NL}-\alpha P_N}(\alpha)/d\alpha = 0$ and is found to be [6]

$$\alpha \approx -\gamma L_{eff} \frac{N+1}{2}.$$

The variance of nonlinear phase noise is given by

$$\sigma^2_{\phi_{NL}} \approx \frac{2\langle \phi_{NL} \rangle^2}{3\rho_s}$$

and the variance of residual nonlinear phase noise is given by

$$\sigma^2_{\phi_{NL}+\alpha P_N} \approx \frac{\langle \phi_{NL} \rangle^2}{6\rho_s}.$$

The reduction in nonlinear phase noise variance is depicted in figure 7 for an SNR of 16.02 dB versus increasing mean nonlinear phase shift which is a function of number of spans in the link. Figure 8 on the next page indicates the performance of linear MMSE compensation through the visual analysis of the received signal PDF before and after compensation.

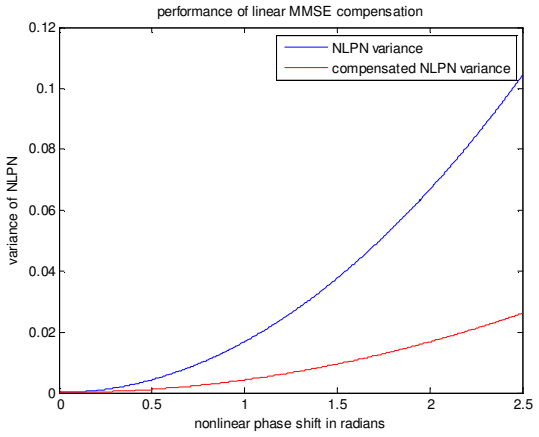

Figure 7: Performance linear MMSE compensator.

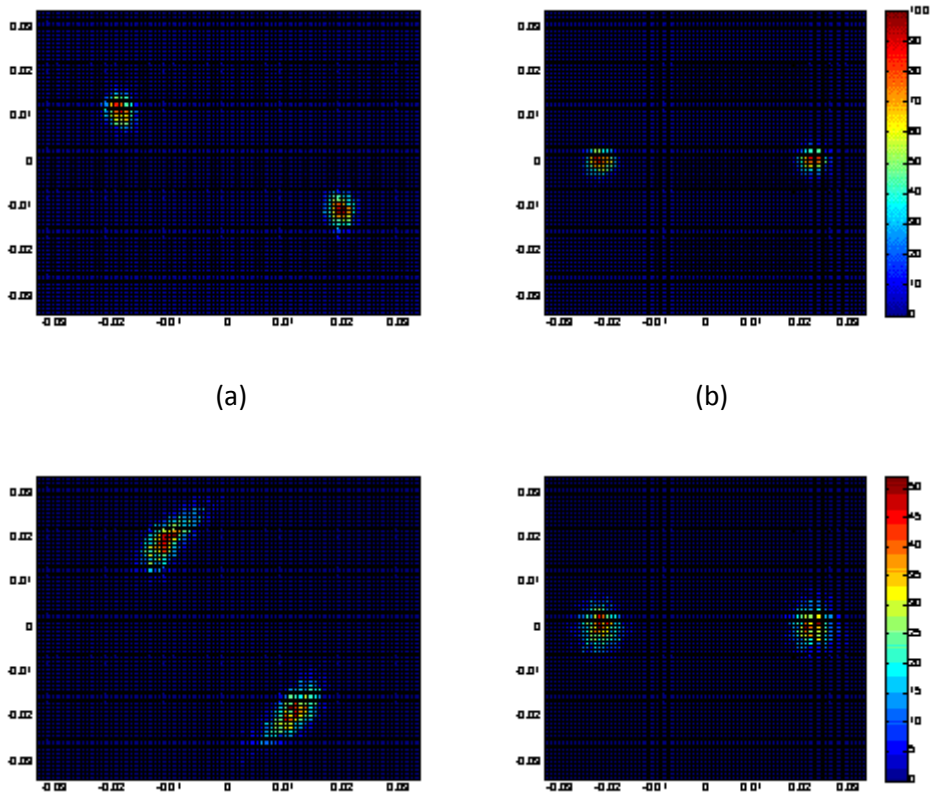

(a) (b)

(c) (d)

Figure 8: Received (a),(c) and compensated (b) (d) PDF for transmitted power of -3 dBm after 4000 km and 8000 km .

Figure 8 clearly shows that the higher the nonlinear phase noise, the higher is the residual nonlinear phase noise variance after compensation as indicative in figures 8(c) and 8(d). Figure 9 on the next page analyzes the effect of NLPN through another prespective. It shows the plot of phases for transmitted symbols and their PDF. It also shows the the compensated phases and their PDF which indicates that the PDF of phase comes back to zero mean after compensation.

Now under the assumption that linear and nonlinear phase noises are independent the total variance of received signal is the sum of both the variances and so the total variance can be expressed as follows:

$$\sigma_{\phi_r}^2 = \sigma_{\theta_n}^2 + \sigma_{\phi_{NL}}^2 \approx \frac{1}{2\rho_s} + \frac{2\langle \phi_{NL} \rangle^2}{3\rho_s}$$

and after linear MMSE compensation the total variance can be expressed as follows:

$$\sigma_{\phi_r}^2 = \sigma_{\theta_n}^2 + \sigma_{\phi_{NL}+\alpha P_N}^2 \approx \frac{1}{2\rho_s} + \frac{\langle \phi_{NL} \rangle^2}{6\rho_s}.$$

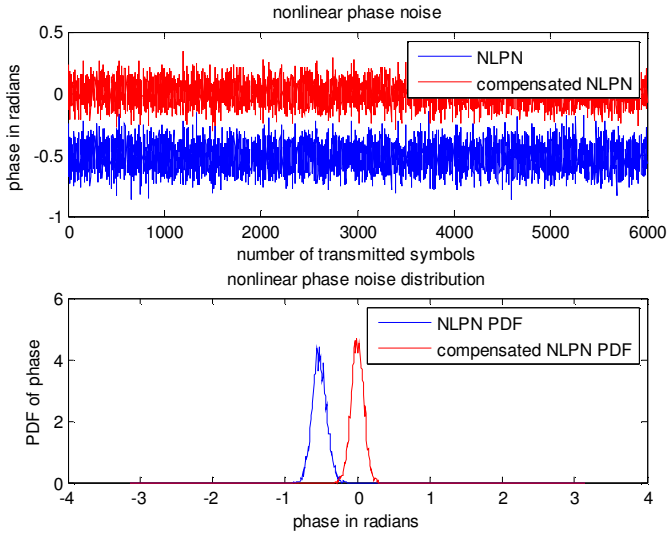

Figure 9: Plot and histogram of NLPN for transmitted power of -3dBm and system length of 4000 km.

Figure 10 compares the theoretical and simulated variances of the total received phase versus propagation distance expressed in number of amplifier spans. The results indicate an almost match between simulated and theoretical variances before and after compensation of NLPN.

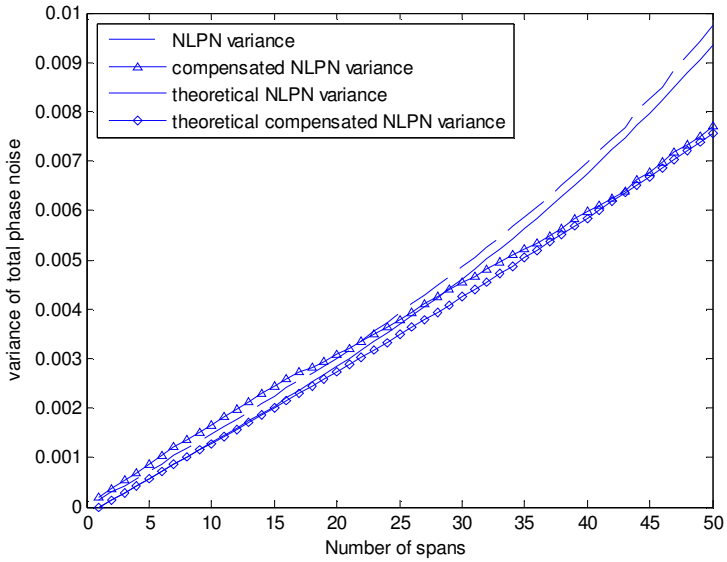

Figure 10: Theoretical and simulated total phase variance for a system length of 4000 km and transmitted power of -3 dBm.

4.6. NONLINEAR MAP COMPENSATION

Nonlinear compensation compensates the NLPN by subtracting from the received phase an optimal phase $\theta_c(r)$ that represents the centre phase which satisfies the following condition [9]

$$f_{P,\theta}(r,\theta_c(r)+\pi/M)=f_{P,\theta}(r,\theta_c(r)-\pi/M)$$

where M is the modulation level, $f_{P,\theta}(r,\theta_r)$ is the joint PDF of the received amplitude r and phase θ_r for a transmitted power P and phase θ as presented in section 3.6 and $[\theta_c(r) \pm \pi/M]$ are the rotated maximum likelihood (ML) boundaries in NLPN. This optimal phase compensator is a nonlinear function of r in the form of

$$\theta_c(r) = c_2 r^2 + c_1 r + c_0$$

and hence a nonlinear compensator. It is also a (maximum a posteriori probability) MAP compensator since the constants c_2, $c_1$and c_0 are functions of the transmitted power P. The constants are formulated in Appendix A.

Figure 11 shows the PDF of a received signal and its ML boundaries for a QPSK signal at an average received power of -4 dBm, for a distance of 5000 km. Figure 12 on the next page shows the PDF of a compensated signal and its ML boundaries. The ML boundaries become straight after compensation which can easily be implemented in the receiver.

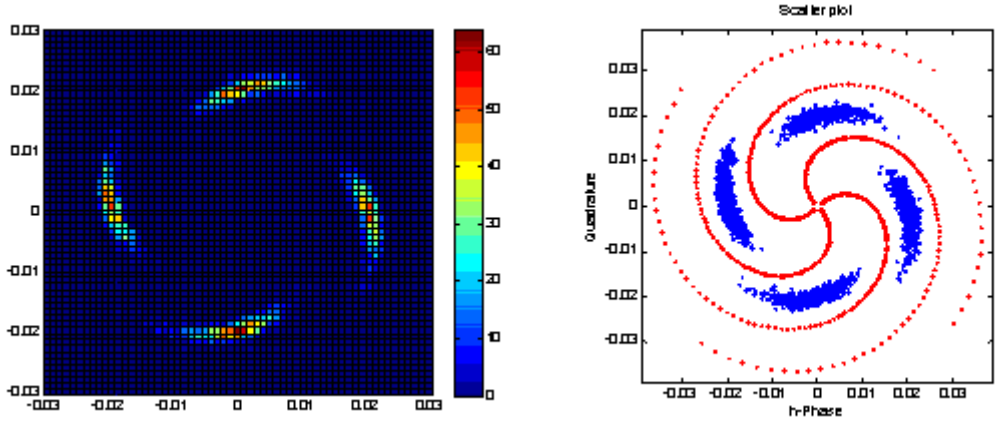

(a) (b)

Figure 11: (a) Received PDF at -4 dBm after 5000 km (b) ML decision boundaries

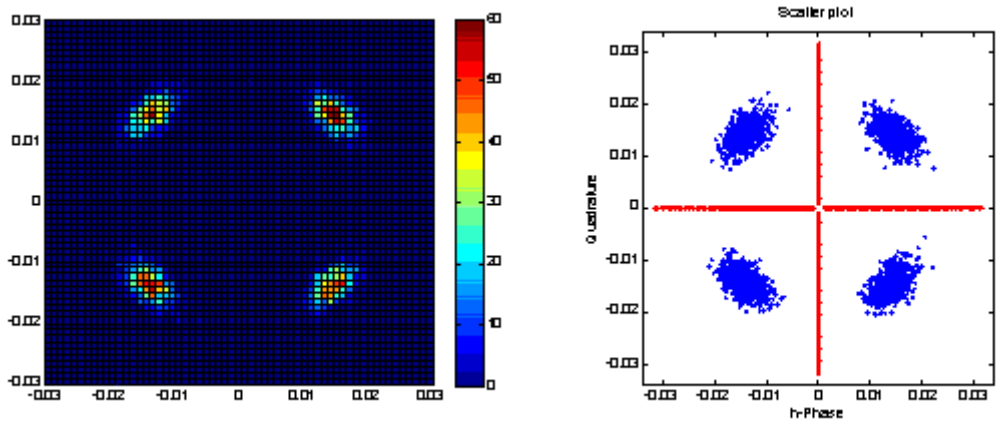

(a) (b)

Figure 12: (a) Compensated PDF at -4 dBm after 5000 km (b) ML decision boundaries.

CHAPTER 5

SIMULATION RESULTS

5.1. SYSTEM MODEL

Table 1 lists the parameters used for simulations .The parameters are same as in [9].

γ	Nonlinear coefficient	$1.2W^{-1}$/Km
Δv_{opt}	Optical filter bandwidth	42.7 GHz
λ	Wavelength	1.55 um
α	Attenuation coefficient	0.25 dB/km
η_{sp}	Spontaneous emission factor	1.41

Table 1: Parameters for simulations.

Attenuation in the fiber is completely compensated by the EDFAs and the ASE noise added to the system is given by $\sigma^2 = 2S_{sp}\Delta v_{opt} = 2hv\eta_{sp}\Delta v_{opt}\alpha L_A$ which has already been defined in section 2.1. The gain of each amplifier is equal to αL_A where L_A is fiber length between each amplifier.

5.2. DISTRIBUTED AMPLIFICATION

In distributed amplifications the signal travelling through the fiber is amplified throughout the fiber length or in other words the system has a uniform amplification throughout the fiber. It can also be assumed as a system with very small incremental lengths between amplifiers and having a large number of amplifiers.

5.3. LUMPED AMPLIFICATIONS

Lumped amplification is practically implemented in long haul fiber optical communication links. Each amplifier is placed at distances from about 40 to 100 kilometers for 10 Gbps systems. The gain of each amplifier is equal the loss in the span between the EDFAs.

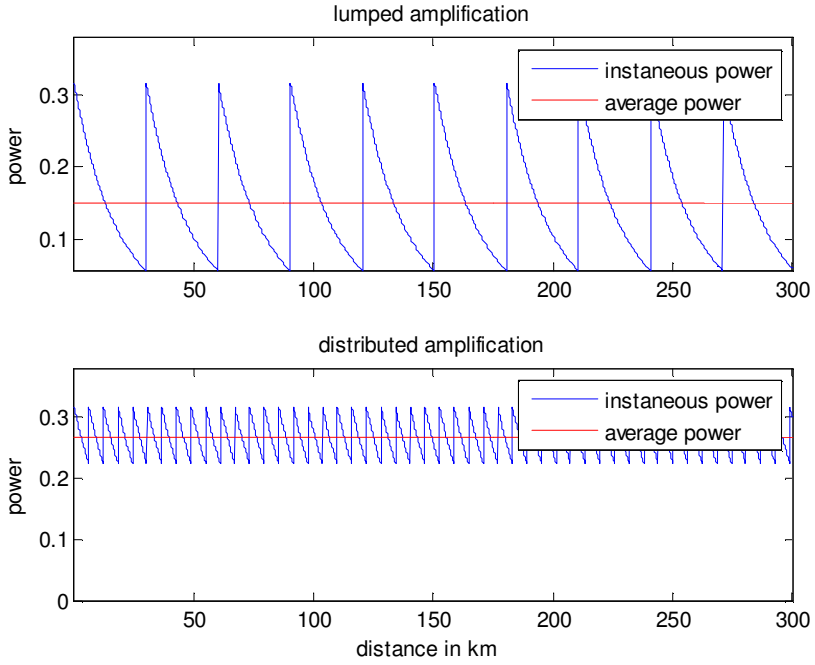

Figure 13: lumped and distributed amplification.

5.4. AVERAGE POWER DEFINITION

The average power travelling through the fiber is given as follows:

$$\overline{P} = \frac{1}{L_A}\int_0^{L_A} P_0 e^{-\alpha z} dz = \frac{1-e^{-\alpha L_A}}{\alpha L_A}$$

where P_0 is the launched power and $\bar{P}$ is the average power travelling through the fiber. In order to maintain the average received power almost equal to that of launched power distributed amplification is used in simulations. Figure 13 illustrates difference between lumped and distributed amplification in terms of powers travelling through the fiber. In lumped amplification, launched power and average power are different where as in distributed amplification launched power and average powers are almost the same indicated by red line.

In [9] distributed amplification model has been used, so the simulations in the thesis work also use distributed amplification.

5.5. BASE BAND SIMULATION

The simulations were carried out by only considering the base band symbols of the modulated signal. Then NLPN noise was added in steps equal to the number of the amplifiers in the system. In the simulations shot noise and thermal noise [1, p.153-154] from the receiver diodes was ignored. Chromatic dispersion was also ignored in the simulations.

5.6. INTERPRETATION OF SIMULATION MODEL

The first step in the simulations was to confirm whether the simulation results match with the theoretical model or not? Here Gaussian approximation of the exact model presented in earlier chapters about linear phase noise and NLPN is used to confirm the simulation model. The received signal is sum of the linear and nonlinear phase noise given by

$$\phi_r = \theta_n + \phi_{NL}$$

where ϕ_r is the total received phase, θ_n is linear phase noise and ϕ_{NL} is NLPN. The distribution of total received phase, approximated by Gaussian distribution is as follows:

$$p_{\phi_r}(\phi_r) = \frac{1}{\sigma_{\phi_r}\sqrt{2\pi}} \exp\left(-\frac{\left(\phi_r - \langle \phi_{NL} \rangle\right)^2}{2\sigma_{\phi_r}^2} \right)$$

Where $\langle \phi_{NL} \rangle$ is the mean nonlinear phase shift and total received phase variance is given by

$$\sigma_{\phi_r}^2 = \sigma_{\phi_{NL}}^2 + \sigma_{\theta_n}^2$$

where $\sigma_{\phi_{NL}}^2$ and $\sigma_{\theta_n}^2$ are the variances of NLPN and linear phase noise. The variances have been quantified in the chapters 3 and chapter 2. Figure 14 shows the received signal PDF of a BPSK modulated signal, with an average received power of -5 dBm and system length of 3000 km which has been used to confirm the Gaussian approximation of the received phase.

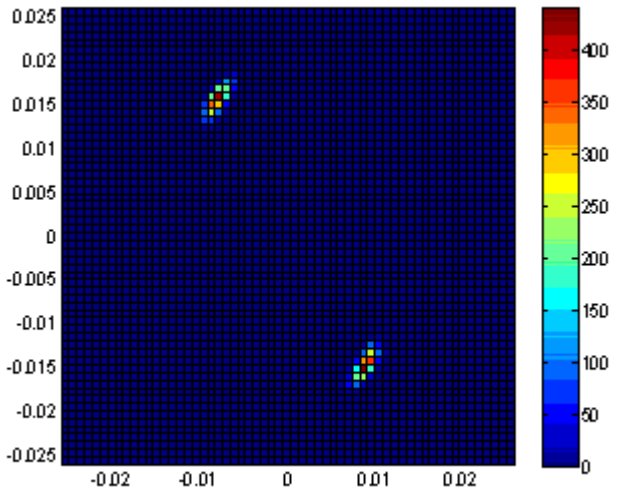

Figure 14: Received signal PDF for a BPSK signal for a system length of 3000 km and average received power of -5 dBm

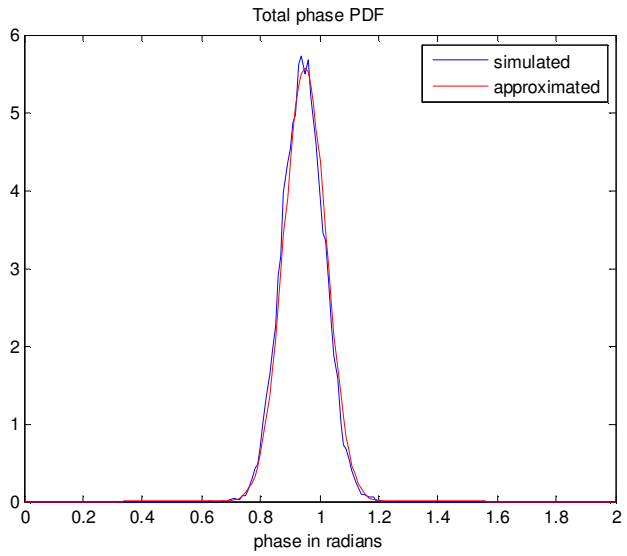

Figure 15: Distribution of total phase of BPSK signal in Figure 14.

Figure 15 shows that there is a good match between the Gaussian approximation and simulated results which confirms the correctness of the simulation model.

In following sections three methods to compensate NLPN are discussed when 16 QAM is used for data transmission.

5.7. PRE COMPENSATION

Pre compensation in [9] is implemented by pre rotating the constellation at the transmitter, by the mean nonlinear phase shift $\langle \phi_{NL} \rangle$. The pre rotation for each point in a square 16 QAM constellation is different since the mean nonlinear phase shift is a function of transmitted amplitude given by $\langle \phi_{NL} \rangle \approx N_A \gamma L_{eff} |A|^2$.

5.8. POST COMPENSATION

Post compensation in [9] is implemented by linear MMSE compensation along with pre compensation at the transmitter. When pre compensation is used along with post compensation the pre compensation is not $\langle \phi_{NL} \rangle \approx N_A \gamma L_{eff} |A|^2$ rather the pre compensation is given by

$$\langle \phi_{NL} \rangle - \left\langle \frac{\gamma L_{eff} P_{rec}}{2} \right\rangle = \langle \phi_{NL} \rangle - \frac{\gamma L_{eff} \left(P_t + \sigma^2 \right)}{2}$$

where P_{rec} is the received power and P_t is the transmitted power and

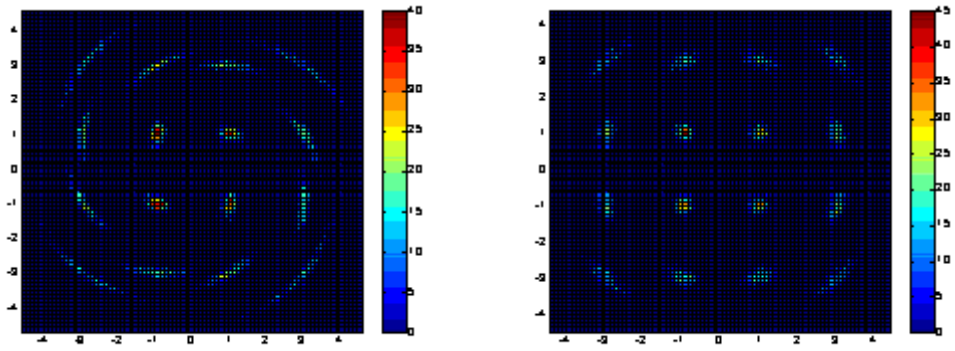

(a) (b)

Figure 16: Received signal PDF after (a) pre compensation and (b) post compensation for system length of 3000 km and at received power of -1 dBm.

$$\left\langle \frac{\gamma L_{eff} P_{rec}}{2} \right\rangle = \left\langle \phi_r - \alpha P_{rec} \right\rangle$$

is the mean of the phase after post compensation given by $\langle \phi_r - \alpha P_{rec} \rangle$. It can be further elaborated in terms of transmitted amplitude A as follows:

$$\langle \phi_{NL} \rangle - \left\langle \frac{\gamma L_{eff} \left| A + n_1 + ... + n_{N_A} \right|^2}{2} \right\rangle = \langle \phi_{NL} \rangle - \frac{\gamma L_{eff} \left(|A|^2 + \sigma^2 \right)}{2}$$

In other words the mean, $\langle \phi_r - \alpha P_{rec} \rangle$ is subtracted from $\langle \phi_{NL} \rangle \approx N_A \gamma L_{eff} |A|^2$ so that the post compensation doesn't over compensate the received signal.

Figure 16 shows the PDF of a 16 QAM signal after pre and post compensation. NLPN is significantly reduced when post compensation is used along with pre compensation, as apparent in figure 16(b).

5.9. NONLINEAR COMPENSATION

A 16 QAM constellation has three shells with three different amplitudes. In order to implement nonlinear compensation discussed in section 4.6 for a 16 QAM signal, the receiver requires the knowledge of transmitted power. This is so because the constants c_2, c_1 and c_0 are functions of transmitted powers. Thus at the receiver 16 QAM received signal is separated into three amplitudes by ML detection to determine the transmitted powers for each received symbol. After this post nonlinear compensation is applied to each received signal depending on the estimated value of transmitted the power.

5.10. COMPARISON OF PHASE AND AMPLITUDE STANDARD DEVIATIONS

As described in section 3.6 the distribution of received amplitudes have Rice distribution which is given by

$$f_R(r,P) = 2re^{-(r^2+P/\sigma^2)} + I_o(2r\sqrt{P/\sigma^2})$$

and the variance of is given by

$$\sigma_r^2 = 2\sigma^2 + r^2 - \frac{\pi\sigma^2}{2} L_{1/2}^2\left(-\frac{r^2}{2\sigma^2}\right)$$

where σ^2 is the variance of ASE noise and $L_{1/2}^2$ is the Laguerre polynomial defined as

$$L_{1/2}^2(x) = e^{x/2}\left[(1-x)I_0\left(\frac{-x}{2}\right) - xI_1\left(\frac{-x}{2}\right)\right]$$

where I_0 and I_1 are the modified Bessel functions of first kind of order 0 and 1.

From section 4.6 the variance of the total received phase is given by

$$\sigma_{\phi_r}^2 = \sigma_{\theta_n}^2 + \sigma_{\phi_{NL}}^2 \approx \frac{1}{2\rho_s} + \frac{2\langle\phi_{NL}\rangle^2}{3\rho_s}$$

A comparison of the variances of the received amplitude and total phase is illustrated in figure 17. From the analysis of figure 17 we observe that at low power levels the OSNR is low, so received amplitudes have high standard deviation. As the transmitted power is increased the OSNR increases resulting in the decrease of standard deviation of the received amplitudes. On the other hand, at high OSNRs the NLPN becomes dominant increasing the standard deviation of the received phase.

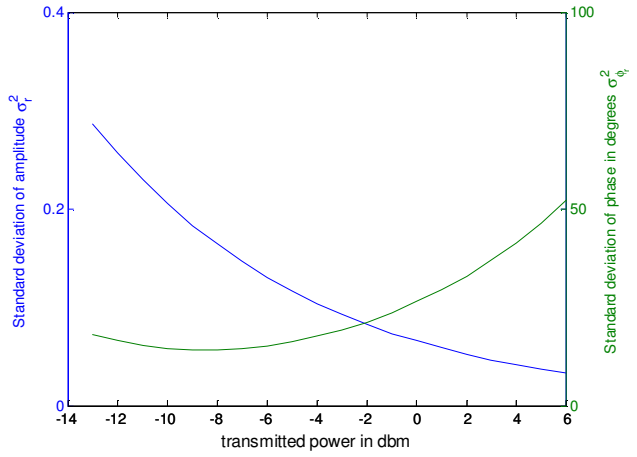

Figure 17 : Comparison of received amplitude and phase standard deviation.

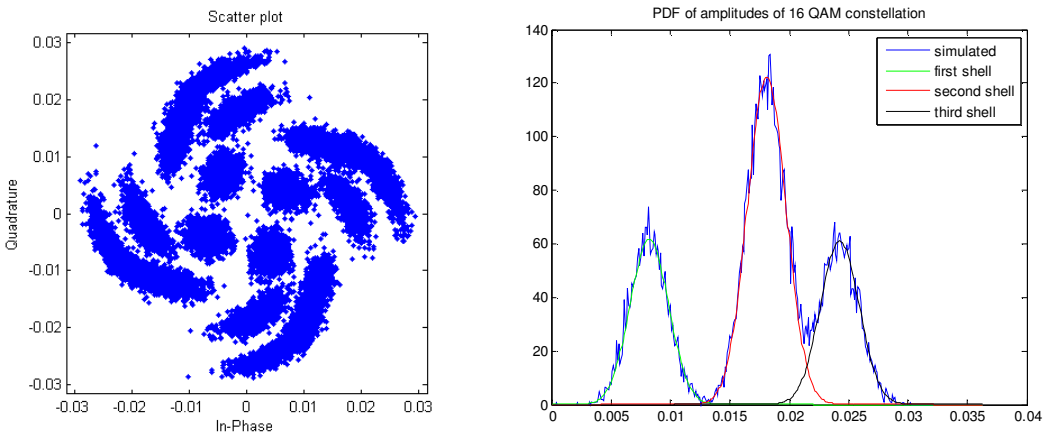

(a) (b)

Figure 18: (a) Received 16 QAM constellation at -5dBm.
(b) Distribution of received amplitudes of 16 QAM Constellation at -5 dBm .

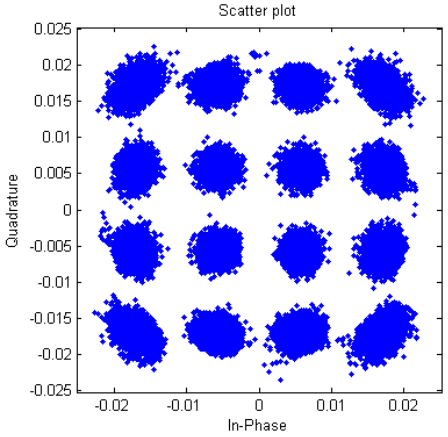

Figure 19: Constellation after nonlinear post compensation at -5 dBm.

Scatter plot of a 16 QAM signal at -5 dBm is shown in figure 18(a). The distribution of amplitudes of the constellation in figure 18(a) is shown in the figure 18(b). From the analysis of figure 18(b) we can observe that the ML detection of the second and third shell amplitudes is erroneous as the PDFs of second and third shell overlap. In such a situation the received signal constellation after nonlinear post compensation is shown in figure 19. We can observe in the scatter plot in figure 19, that some of the points in the second shell are over compensated. This over compensation results in poor performance of nonlinear compensation at low transmitted powers.

5.11. EQUALLY SPACED PHASE CONSTELLATION

In a square 16 QAM constellation the points in the middle shell are not uniformly distributed as shown in figure 20. This results in unequal decision regions due to nonlinear phase noise. So the performance of nonlinear post compensation can be further improved by uniformly distributing the points in the middle shell of a square 16 QAM constellation as shown in figure 20 by dots.

Based on earlier discussion a simple conclusion is drawn that by using a multilevel constellation having uniform distribution in terms of amplitude and phase the performance of the nonlinear post compensation can be further improved.

Keeping in view the square 16 QAM constellation, optimization of 16 QAM constellation is done by uniformly distributing all 16 points in four shells instead of three, keeping the lowest and highest shell radii equivalent to that of square 16 QAM constellation, which are calculated in appendix B. The modified circular 16 QAM constellation along with its ML decision regions is shown in figure 21 on next page.

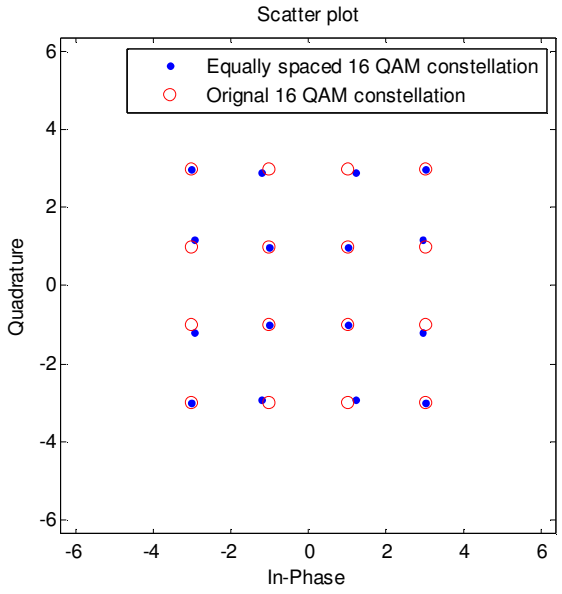

Figure 20: Constellation of square and equal phase 16 QAM constellation.

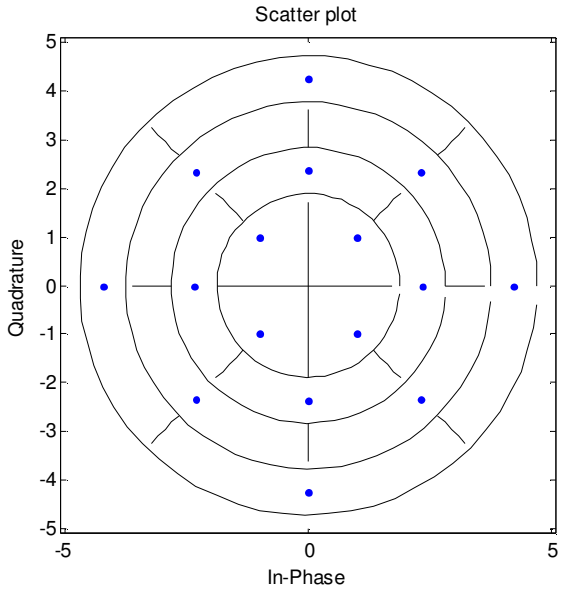

Figure 21: Circular 16 QAM constellation and decision regions.

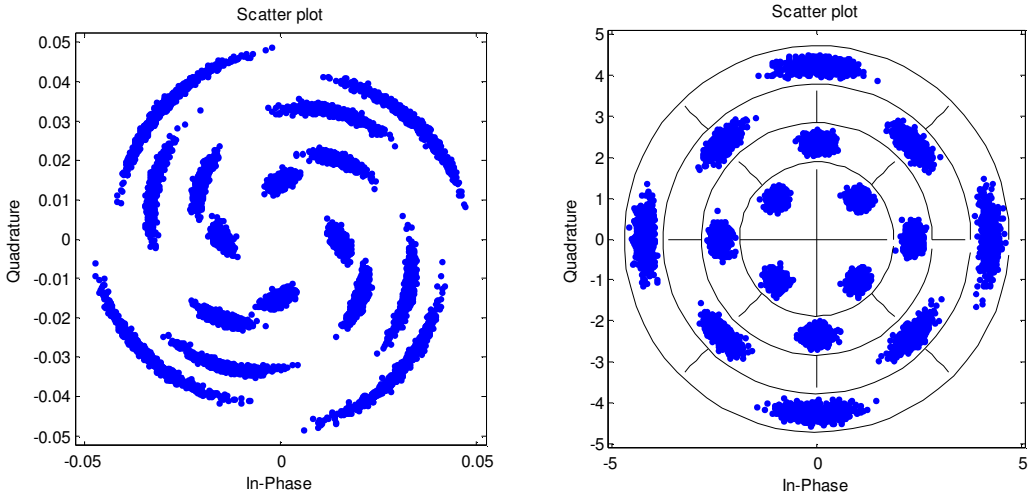

(a) (b)

Figure 22: (a) NLPN in circular 16 QAM (b) Compensated circular 16 QAM Constellation and decision boundaries.

Figure 22(a) illustrates the received constellation of a circular 16 QAM constellation after a propagation distance of 3000 km and average received power of 0 dBm. Figure 22(b) shows the compensated constellation by nonlinear post compensation. From the analysis of figure 22(b) it is apparent that noise has higher variance in terms of phase than amplitude so the decision boundaries are close to ML. The advantage of the these approximate ML boundaries is that they can be easily implemented in the receiver if decisions are made in terms of amplitude and phase since they can be considered as straight decision boundaries in terms of amplitude and phase.

5.12. PERFORMANCE COMPARISON OF NLPN COMENSATION TECHNIQUES

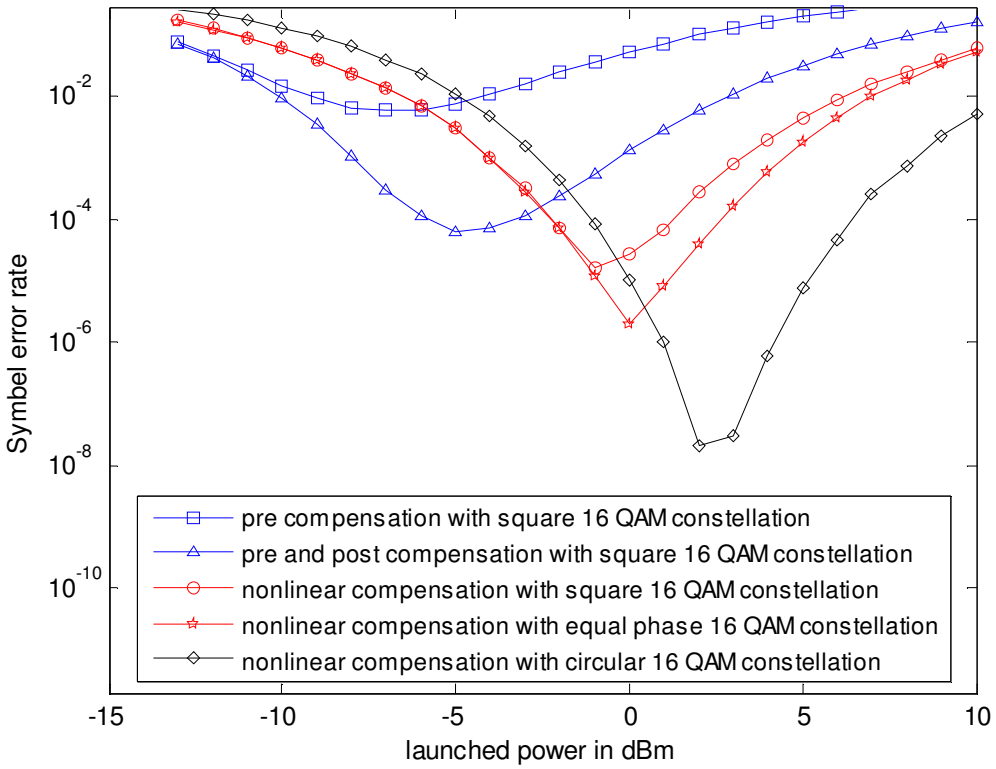

Figure 23: Performance comparison of compensation techniques

Figure 23 compares the performance of compensation techniques for mitigating nonlinear phase noise, for transmission distance of 3000 km and with all constellations normalized at the same transmit energy.

With square 16 QAM constellation, the optimum point of performance for only pre compensation is at -7 dBm. When linear MMSE post compensation is used along with pre compensation the optimum performance point increases to -4 dBm with symbol error rate (SER) at around 10^{-4}. As the transmit power increases the NLPN again comes into play further degrading the performance of the system.

When nonlinear post compensation is used the optimum point of performance is increased to about -1 dBm with SER reduced to 10^{-4}. When equal phase 16 QAM constellation is used the performance of nonlinear compensation is further improved as the optimum point of performance is increased to around 0 dBm with SER reduced to 10^{-6}. This improvement is because nonlinear post compensation assumes uniform ML boundaries in NLPN and the uniform distribution of points in terms of phase implements the assumption.

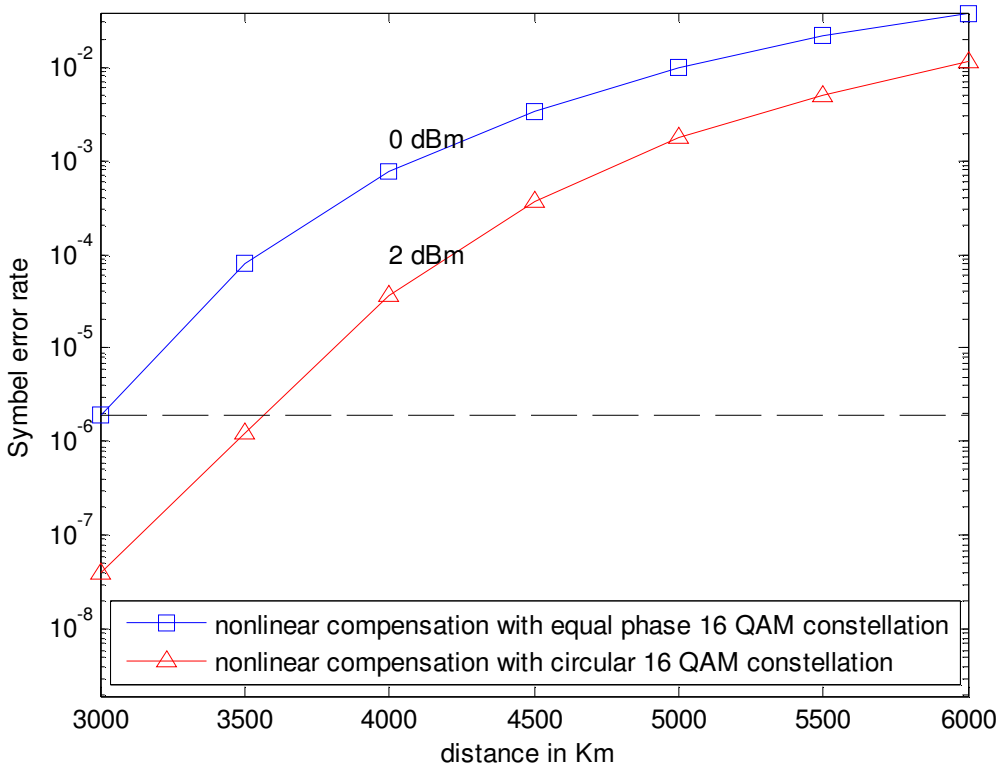

Figure 24: SER versus system length with nonlinear compensation.

After this circular 16 QAM constellation is tested along with nonlinear post compensation. The results achieved are further improved as the optimum point of the performance is pushed to 2 dBm with SER reduced to around 10^{-8}. This improvement is due to two reasons. The circular 16 QAM constellation has a uniform distribution of phases. Secondly introduction of four shells reduces the amplitude of points in second shell thus reducing the total variance of NLPN of the constellation at higher transmit powers.

The key advantage here is that with the same complexity of the receiver, the system becomes more immune to nonlinear phase noise at higher transmitted powers thus enabling the system to transmit data to further distances for the same symbol error probability.

Figure 24 compares the performance of nonlinear post compensation versus increasing system lengths at optimum launched powers of 0 dBm, for equal phase 16 QAM constellation, and 2 dBm for circular 16 QAM constellation. The system length increases from 3000 km to 3540 km for the symbol error rate of 10^{-6} with circular 16 QAM constellation. So the overall advantage in terms of distance is around 540 km for the least SER of 10^{-6} achieved in [9].

CHAPTER 6

FUTURE WORK

6.1. DISPERSION ANALYSIS

Chromatic dispersion causes the signal to spread in time causing the amplitude of the signal pulse to decrease. Since nonlinear phase shift is directly proportional to the signal amplitude so the variance of the nonlinear phase shift should also decrease with increase in chromatic dispersion [14]. A similar conclusion has also been drawn in [15] but with a different mathematical approach.

But the above results have been contradicted in [16] as no role of Intra Cross Phase Modulation (IXPM), due to inter symbol interference as a result of chromatic dispersion, has been considered.

For future work it would be a good task to analyze the behavior of interplay of nonlinear phase noise and chromatic dispersion as well as statistically modeling the NLPN in that case.

6.2. CODING ANALYSIS

For the analysis of symbol error probability of a 16 QAM constellation, noise is considered to be Gaussian and having same variance in the two degrees of freedom for all the points in the constellation [17]. But from the analysis of figure 22(a) and figure 22(b) we observe that higher signal amplitudes have higher variance of nonlinear phase noise. It clearly indicates that an imbalanced error control coding scheme is required that encodes the data with higher signal amplitudes with more powerful codes than the ones with low signal amplitudes.

So an imbalanced but optimized error control coding scheme can further improve the system performance or in other words by optimizing the over head of error control coding scheme the bit error rate can be further reduced.

For future it would be an interesting task to optimize the previously proposed error control coding schemes for fiber optical communication in the context of nonlinear phase noise in the system.

REFERENCES

1. Govind P. Agrawal ,``Light Wave Technology Telecommunication Systems´´, 2nd Edition, John Wiley & Sons,2005.

2. Keang-Po Ho, ``Phase-Modulated Optical Communication Systems", Springer, 2005.

3. Rodger E. Ziemer, Roger L. Peterson, ``Introduction to digital communication'', 2nd Edition, Prentice Hall, 2001.

4. http://www.rp-photonics.com/nonlinear_index.html, April, 2009.

5. J. P. Gordon and L. F. Mollenauer, ``Phase noise in photonic communications systems using linear amplifiers", Optics Letters, Vol. 15, No. 23, pp. 1351-1353,December 1, 1990.

6. Keang-Po Ho, Joseph M. Kahn, ``Electronic Compensation Technique to Mitigate Nonlinear Phase Noise", Journal of light wave technology, vol. 22, No. 3, pp. 779, March 2004.

7. Keang-Po Ho, ``Asymptotic probability density of nonlinear phase noise'', Optics Letters, Vol. 28, No. 15, pp. 1350-1352, August 1, 2003.

8. Keang-Po Ho, ``Performance Degradation of Phase-Modulated Systems due to Nonlinear Phase Noise'', IEEE Photonics Technology Letters, VOL. 15, No. 9, pp. 1213-1215, September 2003.

9. Alan Pak Tao Lau and Joseph M. Kahn, ``Signal Design and Detection in Presence of Nonlinear Phase Noise". Journal of Lightwave Technology, Vol. 25, No. 10, pp. 3008-3016, October 2007.

10. Ezra Ip, Alan Pak Tao Lau, Daniel J. F. Barros and Joseph M. Kahn, ``Compensation of Dispersion and Nonlinear Impairments Using Digital Backpropagation", Journal Of Lightwave Technology, Vol. 26, No. 20,pp. 3416-3425, October 15, 2008.

11. Per Kylemark, ``Nonlinear Fiber Optical Technologies for Transmission and Amplification" Technical report - Department of Micro technology and Nano Science, Chalmers University of Technology, 2004.

12. Govind P. Agrawal, ``Nonlinear Fiber Optics'', 4th Edition, Academic Press,2006.

13. Ezra Ip and Joseph M. Kahn, ``Increasing Optical Fiber Transmission Capacity beyond Next-Generation Systems", IEEE Lasers and Electro-Optics Society, 2008. LEOS 2008. 21st Annual Meeting, pp. 606-607, November 9-13, 2008.

14. Shiva Kumar, ``Effect of dispersion on nonlinear phase noise in optical transmission systems´´ Optics Letters, Vol. 30, No. 24, pp. 3278-3280, December 15, 2005.

15. A G. Green and P. P. Mitra, L. G. L. Wegener, `` Effect of chromatic dispersion on nonlinear phase noise", Optics Letters, Vol. 28, No. 24, pp. 2455-2457, December 15, 2003.

16. Keang-Po Ho, Hsi-Cheng Wang, ``Effect of dispersion on nonlinear phase noise", Optics Letters, Vol. 31, No. 14, pp. 2109-2111 ,July 15, 2006.

17. Erik Strom, ``Notes on Quadrature Amplitude Modulation", Lecture notes in digital communications course, course code (SSY-125), Chalmers University of Technology Sweden, November 7, 2005.

APPENDIX A

The detailed expression for nonlinear post compensation $\theta_c(r) = c_2 r^2 + c_1 r + c_0$ from [9] is presented in this appendix and it refers to section 4.6 and 5.9 in the main text.

$$\theta_c(r) = \sqrt{\frac{x}{2}} \frac{\sin\sqrt{2x} - \sinh\sqrt{2x}}{\cosh\sqrt{2x} - \cos\sqrt{2x}} r^2 - 4\sqrt{\frac{\rho_s x}{2}} \frac{\sin\sqrt{\frac{x}{2}}\cosh\sqrt{\frac{x}{2}} - \cos\sqrt{\frac{x}{2}}\sinh\sqrt{\frac{x}{2}}}{\cosh\sqrt{2x} - \cos\sqrt{2x}} r + h(x, \rho_s)$$

Where $\rho_s = \frac{|A|^2}{2N_A\sigma^2}$ is the OSNR and $h(x, \rho_s)$ is defined as follows:

$$h(x, \rho_s) = -\frac{\pi}{4} + \tan^{-1}\left(\cot\sqrt{\frac{x}{2}}\tanh\sqrt{\frac{x}{2}}\right) - \rho_s\sqrt{\frac{x}{2}}\frac{\sin\sqrt{2x} + \sinh\sqrt{2x}}{\cosh\sqrt{2x} + \cos\sqrt{2x}} + 4\rho_s \frac{\sin\sqrt{2x}\cosh\sqrt{2x} - \cos\sqrt{2x}\sinh\sqrt{2x}}{\cosh 2\sqrt{2x} - \cos 2\sqrt{2x}}$$

and x is defined as follows:

$$x = \frac{\gamma P L}{\rho_s + 0.5}$$

where P and L are the transmitted powers and system lengths.

APPENDIX B

The calculations for the radii of modified circular 16 QAM constellation are presented in this appendix and they are referred to section 5.11 in the main text.

Radius of shell 1 in square 16 QAM constellation is given by $r1 = \sqrt{1^2 + 1^2} = \sqrt{2}$

Radius of shell 2 in square 16 QAM constellation is given by $r2 = \sqrt{1^2 + 3^2} = \sqrt{10}$

Radius of shell 3 in square 16 QAM constellation is given by $r3 = \sqrt{3^2 + 3^2} = \sqrt{18} = 3\sqrt{2}$

Difference of radius 1 and radius 3 of square 16 QAM constellation = $\Delta r = r3 - r1 = 3\sqrt{2} - \sqrt{2} = 2\sqrt{2}$

Radius of 1st shell of circular 16 QAM constellation = $r1' = \sqrt{2}$

Radius of 2nd shell of circular 16 QAM constellation = $r2' = \frac{\Delta r}{3} + r1' = \frac{2\sqrt{2}}{3} + \sqrt{2} = \frac{5\sqrt{2}}{3}$

Radius of 3rd shell of circular 16 QAM constellation = $r3' = \frac{\Delta r}{3} + r2' = \frac{2\sqrt{2}}{3} + \frac{5\sqrt{2}}{3} = \frac{7\sqrt{2}}{3}$

Radius of 4th shell of circular 16 QAM constellation = $r4' = r3 = 3\sqrt{2}$